

### 5.4.7 Recipe for the Deadtime Correction

For reference here is equation (5.2)

$$P_j^{noise} = P_1 + P_2 \cos \frac{2\pi j}{N}, \quad (5.2)$$

and (5.3)

$$P_j^{diff} = \Delta P_1 + \Delta P_2 \cos \frac{2\pi j}{N}, \quad (5.3)$$

where  $\Delta P_1 = P_1^{sd} - P_1^d$  is the difference in  $P_1$  coefficients, obtained by fitting power spectrum of the simulated data and the calibration data, respectively, and  $\Delta P_2 = P_2^{sd} - P_2^d$  is the difference in  $P_2$  coefficients.

### Incident Rate Correction

In the absence of the background, for the on-ground calibration data, the incident rate can be calculated from the observed rate using

$$r_{in} = \frac{r_o}{1 - r_o \tau_0}, \quad (5.4)$$

where  $\tau_0 = 16.383 \pm 0.004 \mu s$  is detector 0 deadtime. This is a formula for non-extended deadtime, and it is applicable since the deadtime Monte Carlo model assumes non-extended deadtime with the same time events that do not change the counting rate. For the purpose of the rate correction, the accuracy of the model is sufficient.

In the case of USA operation in orbit, when background rates become significant, the formula for the rate correction should take into account those rates. In this case, the incident rate can be estimated as

$$r_{in} = \frac{r_o}{1 - DTF}, \quad (5.5)$$

where  $DTF$  is a dead time fraction

$$DTF = r_o \tau_0 + r_p \tau_{logic} + r_c \tau_{one-shot} + r_{LE} \tau_{LE}, \quad (5.6)$$

where  $r_p$  is perimeter veto rate,  $\tau_{logic} = 7.5 \pm 1 \mu s$  is perimeter veto deadtime,  $r_c$  is total coincidence veto rate,  $\tau_{one-shot}$  is a deadtime caused by coincidence events ( $\tau_{one-shot}$  is on average  $15.6 \mu s$ , see Section 5.1.1.) ,  $r_{LE}$  is large energy events rate, and  $\tau_{LE}$  is a deadtime caused by these events ( $\tau_{LE}$  varies with the energy of the event, see Section 5.1.1.). This formula is true if all the incident events are independent and can be applied only to the sources with less than 10% deadtime [108]. This formula should be verified by the analysis of the on-orbit calibration data. Note that the value of  $r_{LE}$  is not available and has to be estimated.

### Power Spectrum Correction

In this section we discuss how the power spectrum of a source can be corrected for the noise, based on the findings of the previous sections. The relevant theory is discussed in Section 4.2.3.

It is likely that the power spectrum of the on-orbit calibration data will be different from the power spectrum of the on-ground calibration data. The methods described in this section are useful for the comparison of the on-ground calibration data to the on-orbit calibration data. Section 5.6 describes what calibration needs to be done on-orbit. Similar correction methods need to be developed based on the on-orbit calibration data analysis. The corrections discussed in this section ignore the energy-dependent instrumental effect, and should be applied when the effect is insignificant. The correction methods of this section lay out the basis for the final correction method that considers the energy-dependent effect (Section 5.5).

The most accurate method one can use to correct the source power spectrum for noise is to subtract the same average rate calibration data power spectrum, which is defined by coefficients  $P_k$ . Section 5.4.3 discusses how the power spectrum of the calibration data is described by the set of coefficients  $P_k$ . Despite the accuracy, this method has a very limited application. Since the power spectrum depends on the bin size, the method is not convenient to use for a different binning than the one used in the table 5.3 (Although raw calibration data is available and can be binned as desired). The power spectrum is also rate-dependent. We only have on-ground calibration data for five different rates for detector 0, and for only two of these is the amount of data large (4075 Hz and 4030 Hz). It is unclear how to interpolate these results for other rates without losing accuracy. Thus, this method can only be used for rates close to the rates of the calibration data. This method is very useful for the comparison of the on-ground calibration data to the on-orbit calibration data with the same rates. Two coefficients are sufficient when the bin size is greater than or equal to the deadtime. Table A.1 provides the values of  $P_1$  and  $P_2$  for several values of  $t_b$  and available values of  $r_o$ .

The most general way to correct the power spectrum is to use the Monte Carlo model of Section 5.4.1. The model can be used for the Monte Carlo simulation of the Poisson noise power spectrum and subsequent subtraction from the power spectrum of the data (the simulation and the data should have the same average rate). It can also be used for the simulation of the celestial X-ray source timing behavior and comparison with the observed power spectrum of the source. The advantage of the model is that it can be used

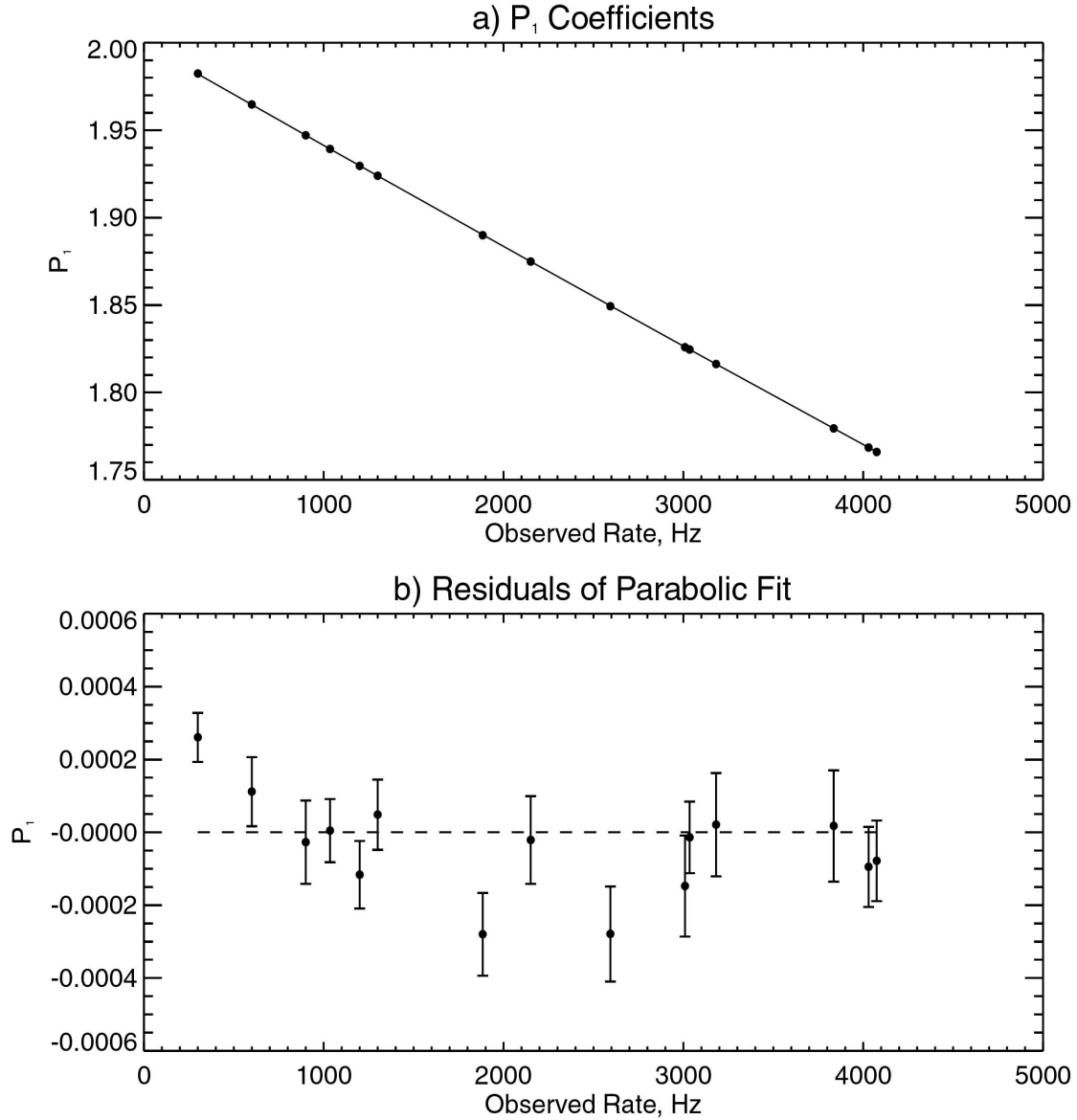


Figure 5.29 a) Parabolic fit to the coefficients  $P_1$  for the simulated data. The error bars are omitted, since they are smaller than the size of the data points. b) Residuals of the fit.  $t_b = 96 \mu\text{s}$ . The deadtime used in the simulation at all rates is the detector 0 deadtime.

for any rate less than 4100 Hz and for any binning. (At rates higher than 4100 Hz it is unclear by how much the model deviates from the data). The deviations of the deadtime

model from the data can be estimated for various rates and values of  $t_b$  (see Section 5.4.6). For some specific parameters, these deviations are known exactly. Table A.3 lists the values of  $P_1$  and  $P_2$  for the simulated data power spectrum for some specific parameters. Combining information from Table A.2 and Table A.3, we can obtain the value of function (5.3), which describes the deviations for these parameters. Even in the situations when we need to know the power spectrum with an accuracy better than the model can provide, we should keep in mind that the deviations of the model from the data have specific functional form (5.3) that can be distinguished from physical phenomena, for example QPOs.

The use of the model requires Monte Carlo simulation of a sufficient number of events. For convenience, we interpolated the  $P_k$  coefficients of simulated data for various rates and binning with a parabola. Figure 5.29 shows the parabolic least squares fit to the  $P_1$  values and the residuals of the fit in the 0-4100 Hz rates range. Figure 5.30 shows the parabolic least squares fit to the  $P_2$  values and the residuals of the fit in the same range. Table 5.6 and Table 5.7 list the results of the fits for various binning. The values in the table 5.6 and table 5.7 can be used to calculate  $P_1$ ,  $P_2$ , and the noise power spectrum according to (5.2). The deviations of the values of  $P_k$  obtained by the interpolation from the ones describing the model are much smaller than the deviations of the model from the data (see figure 5.29b).

For low rate sources, a convenient method to describe the power spectrum of the noise is to use the analytical formula for extended deadtime

$$P_j^{noise} = P_1 + P_2 \cos \frac{2\pi j}{N} = \left[ 2 - 4r_o\tau_0 \left( 1 - \frac{\tau_0}{2t_b} \right) \right] - 2 \frac{N-1}{N} r_o\tau_0 \left( \frac{\tau_0}{t_b} \right) \cos \frac{2\pi j}{N}. \quad (5.7)$$

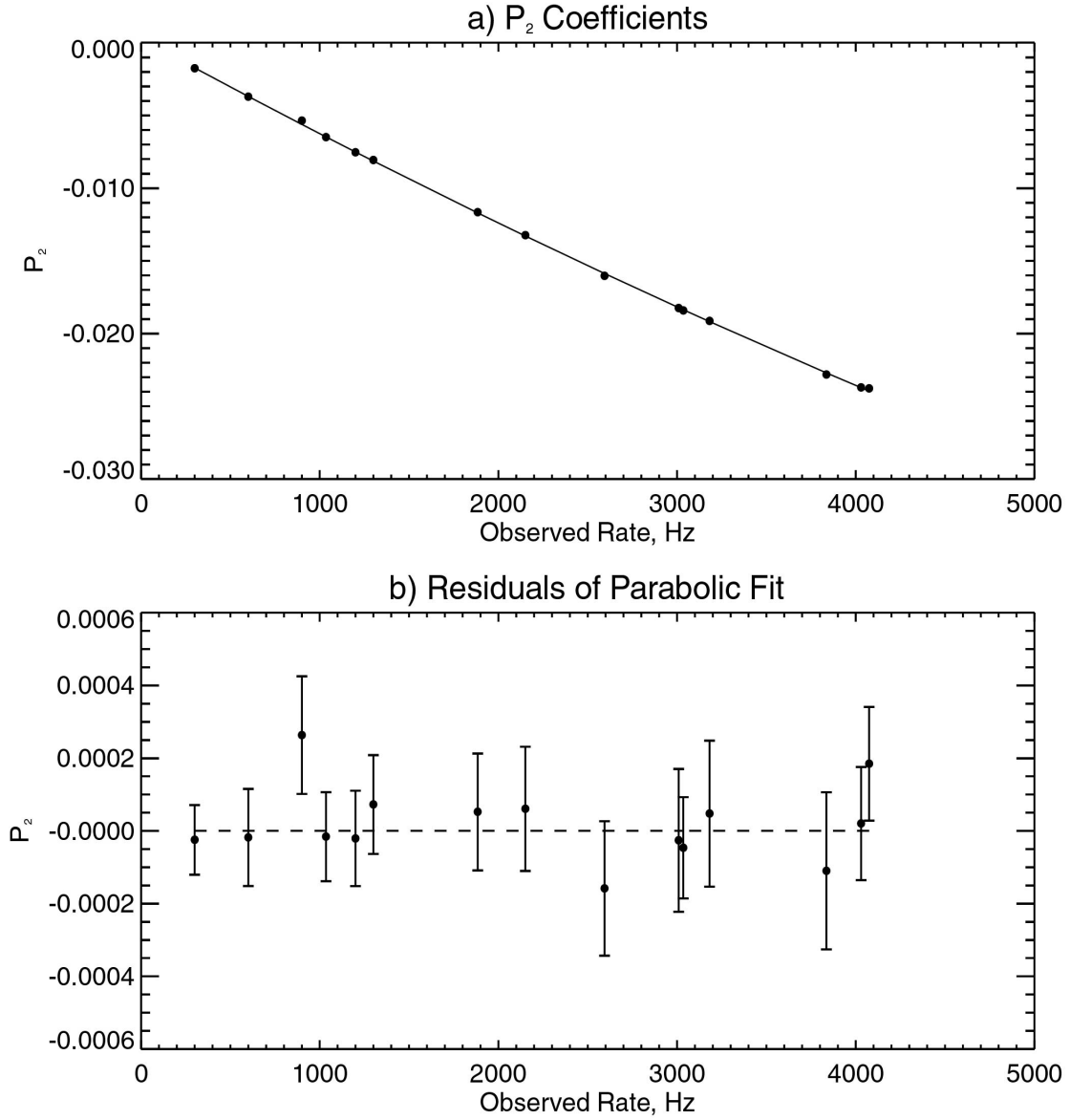


Figure 5.30 a) Parabolic fit to the coefficients  $P_2$  for the simulated data. The error bars are omitted, since they are smaller than the size of the data points. b) Residuals of the fit.  $t_b = 96 \mu\text{s}$ . The deadtime used in the simulation at all rates is the detector 0 deadtime.

$t_b$ ( $\mu$ s)	A	b	c	$\chi^2 / \text{dof}$
32	$(2.20 \pm 0.02) \times 10^{-10}$	$(-4.6432 \pm 0.0005) \times 10^{-5}$	$2.00002 \pm 0.00001$	0.281
96	$(3.7 \pm 0.1) \times 10^{-10}$	$(-5.886 \pm 0.003) \times 10^{-5}$	$1.99977 \pm 0.00004$	2.048
960	$(5.2 \pm 0.4) \times 10^{-10}$	$(-6.497 \pm 0.009) \times 10^{-5}$	$2.0000 \pm 0.0001$	0.703

Table 5.6 Results of the parabolic fit.  $P_1 = ar_o^2 + br_o + c$  . 13 dof.

$t_b$ ( $\mu$ s)	a	b	c	$\chi^2 / \text{dof}$
32	$(3.10 \pm 0.03) \times 10^{-10}$	$(-1.9090 \pm 0.0008) \times 10^{-5}$	$(-4. \pm 2.) \times 10^{-5}$	0.663
96	$(1.9 \pm 0.2) \times 10^{-10}$	$(-6.70 \pm 0.04) \times 10^{-6}$	$(2.6 \pm 0.6) \times 10^{-4}$	0.184
960	$(8. \pm 5.) \times 10^{-11}$	$(-1.0 \pm 0.1) \times 10^{-8}$	$(2. \pm 2.) \times 10^{-4}$	0.684

Table 5.7 Results of the parabolic fit.  $P_2 = ar_o^2 + br_o + c$  . 13 dof.

This formula is convenient to use, because the power spectrum can be calculated for any value of rate and bin size. However, generally, this method is much less accurate than the methods described above. Figure 5.31 shows the difference between the  $P_k$  coefficients for the model and the ones calculated using (5.7) with  $t_b = 96 \mu$ s. At low rates, the discrepancy between the model and the system with extended deadtime decreases. For rates below  $\sim 500$  Hz, the discrepancy between the power spectrum described by (5.7) and the power spectrum of the simulated data is the same as between the power spectrum of the simulated data and the calibration data. We recommend using the extended deadtime formula for low rates if the accuracy is sufficient.

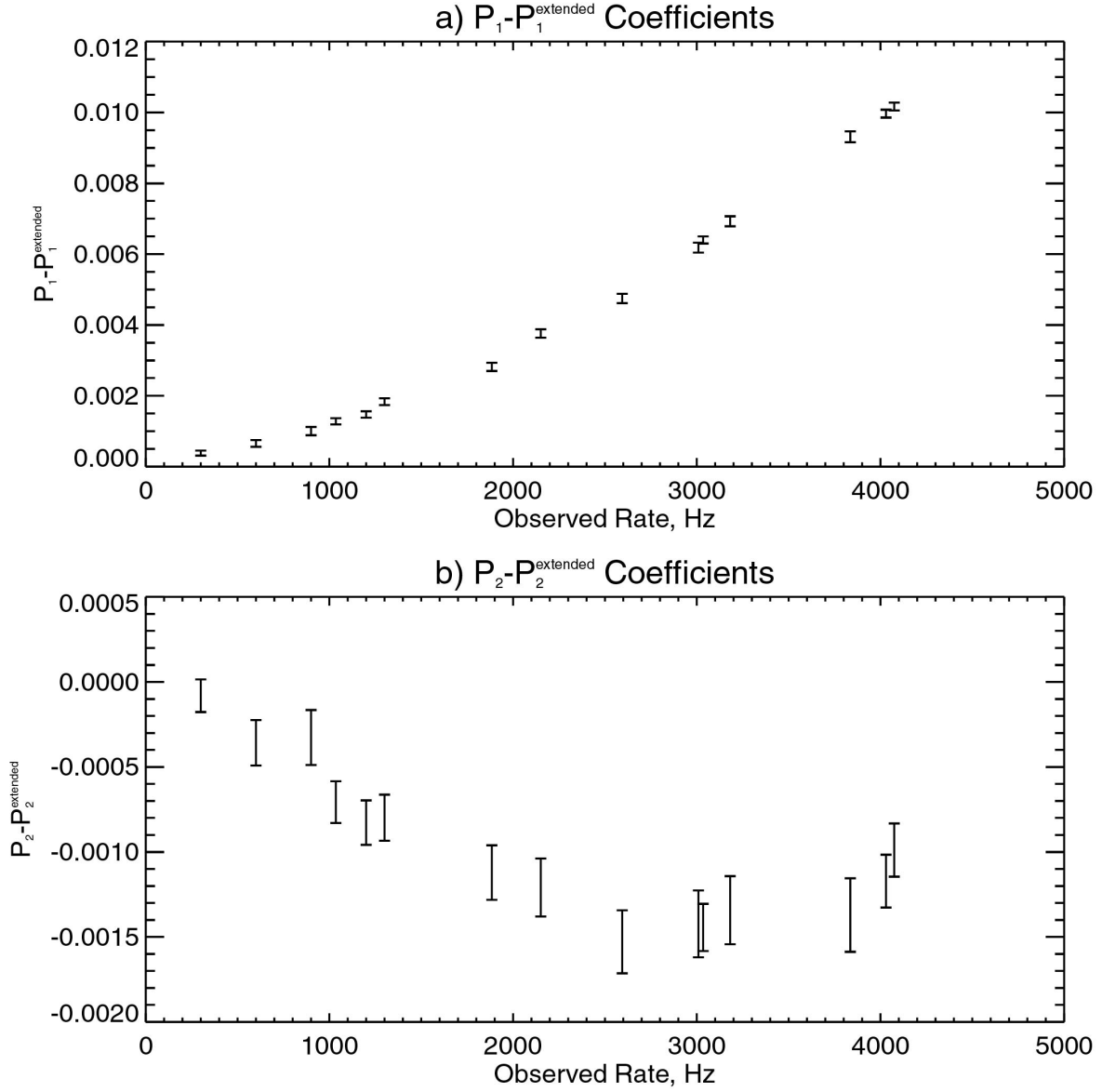


Figure 5.31 a)  $P_1 - P_1^{\text{extended}}$  coefficients. Points with error bars correspond to the simulated data.  
b)  $P_2 - P_2^{\text{extended}}$  coefficients.  $t_b = 96 \mu\text{s}$ . The deadtime used in the simulation at all rates is the detector 0 deadtime.